Hindawi
Advances in Civil Engineering
Volume 2019, Article ID 4201842, 10 pages
https://doi.org/10.1155/2019/4201842

Research Article

Experiments on Reducing Negative Skin Friction of Piles

Zhongju Feng, Haibo Hu, Ruixin Zhao, Jingbin He, Yunxiu Dong, Kai Feng, Yawan Zhao, and Huiyun Chen

School of Highway, Chang'an University, Xi'an, Shaanxi 710064, China

Correspondence should be addressed to Haibo Hu; huhaibo@chd.edu.cn and Jingbin He; Hejingbin_0407@163.com

Received 31 July 2019; Revised 23 October 2019; Accepted 5 November 2019; Published 3 December 2019

Academic Editor: Dimitris Rizos

The objective of this study was to investigate the effect of different moisture contents of clay (13%, 15%, 17%, 19%, and 21%) and different coatings on the ability to reduce negative skin friction during a large-scale shear test. Four coating treatments of the concrete surface were investigated, i.e., no treatment, coating with a paraffin-oil mixture, coating with a polymer nanomaterial, and coating with paint. The results showed that when the moisture content of the clay was slightly larger than that of the plastic limit, the ability to reduce negative skin friction was the best, and the performance was similar for the paraffin-oil mixture, the polymer nanomaterial, and the paint. When the moisture content of the clay was lower than that of the plastic limit, the paraffin-oil mixture provided the best performance. The position of the neutral point can be determined by different methods, and the negative skin friction of piles should be reduced by applying coatings that are most suitable to different conditions.

1. Introduction

With the development of geotechnical engineering, the role of piles is becoming increasingly important [1–4]. The negative skin friction of piles occurs because the settlement deformation of the soil near the pile is larger than that of the pile body [5–8]. The main reasons for the negative skin friction of piles include mass stowage of the ground near the pile [9, 10], ground subsidence caused by loess subsidence, melting of permafrost, and other reasons [11–14]. The negative skin friction does not only become part of the bearing capacity of the pile but is also converted into the external load applied to the pile [15, 16]. In addition, the existence of negative skin friction may cause the pile to settle more than other piles that are not subject to negative skin friction, which will affect the overall safety of the bridge.

In essence, the negative skin friction of piles depends on the interface characteristics between the pile and soil. Uesugi and Kishida [17] investigated the characteristics of the interface between steel plates and sand and found that the sand type and the surface roughness of the steel had large influences on the friction. Poulos [18] found that the pile foundation density, over-consolidation rate, and soil compressibility affected the friction performance. Pincus et al. [19] analyzed the skin friction of piles in sands using a series of experiments; it was concluded that the reduction of the shaft friction should be taken into account in offshore piles and drilled shafts. Chaney et al. [20] found that the skin friction of driven piles at the pile-soil interface was low in calcareous soils due to the reduction in normal effective stresses during the installation of the piles. Kim et al. [21] analyzed the pile-soil interface using a numerical procedure; it was found that using suitable pile material for the pile-soil systems was important. Ampera and Aydogmus [22] determined the magnitude of skin friction between soils and construction materials; it was found that rough concrete had better friction resistance to peat than smooth concrete. Cao et al. [23] used a load transfer model to describe the behavior of the pile-soil interface; it was found that the friction along the piles varied during consolidation and the pile-soil interface was subjected to complex shear. Donna et al. [24] studied the behavior of the pile-soil interface to predict the response of floating piles; it was found that the interface characteristics were not affected directly by the temperature but rather by cyclic degradation. Bersan et al. [25] conducted

a static load test to estimate the properties of the pile-soil interface; the results were used for design validation.

Different methods to mitigate the negative skin friction of piles include prepressure to reduce soil settlement when constructing a pile foundation, using a casing to avoid direct contact between the pile and soil, and using coatings such as bituminous materials to minimize the skin friction between the pile and soil [26–30]. The latter method is widely used and is the most cost effective. However, bituminous materials are temperature-sensitive. At low temperatures, they tend to exhibit solid traits, whereas, at high temperatures, they exhibit fluid traits [31–33]. As the temperature changes, bituminous materials become unstable and are unable to reduce the negative skin friction of piles. Therefore, it is necessary to explore temperature-insensitive coatings to reduce the negative friction resistance of piles.

Considering the above state and taking clay as the test soil, large-scale shear tests were carried out to study the reduction of negative skin friction by the paraffin-oil mixture, polymer nanomaterial and paint. The influences of the moisture content and different coatings on the ability to reduce the negative skin friction were investigated, and measures to reduce the negative skin friction of the pile under different conditions were proposed to provide guidance for engineering practice.

2. Materials and Methods

2.1. Test Equipment. Due to the time and cost requirements of field tests, a large-scale shear test was designed to simulate a field test, and the ratio of the test model to real objects is 1 : 1. The test equipment of the large-scale shear test was provided by Chang'an University, which is located in Xi'an City, Shaanxi Province, China. The test equipment is shown in Figure 1. The pedestal, model A, and model B are made of steel. The two rollers above the pressure plate are made of iron rods and the sliding plates are also made of steel. A sensor and a vertical jack are placed above the sliding plate, and a sensor and a horizontal jack are placed in the horizontal direction of model B. The sensors are connected to an automatic data analyzer. Model A has a bottom plate but no top plate. Model B has no top and bottom plates. The specific model dimensions are shown in Figure 2 with a dimensional unit of mm. Model A is placed at the bottom, where the concrete is located, and different materials are applied to the concrete surface according to different working conditions. Model B is located above model A, where the soil samples with different moisture contents are placed.

According to the sectional shape, piles can be divided into square piles, round piles, heterogeneous piles, and so on. In the test design, the contact surface between the pile and soil is a plane, which can simulate square piles very well. However, in practical engineering, the contact between the pile and soil is always a curved surface. Since the frictional resistance is determined by the nature of the contact interface and the positive pressure and the shape does not have much effect, the results of this experiment can still provide reference for piles of other shapes.

2.2. Materials. The soil samples used in this study were clay derived from Xi'an, Shaanxi. The main physical properties were tested by ring knife tests (Figure 3(a)), oedometer tests (Figure 3(b)), moisture content tests (Figure 3(c)), liquid limit and plastic limit tests (Figure 3(d)), and direct shear tests (Figure 3(e)). The density was calculated with the ring knife tests, in which the ratio of the mass of the soil inside the ring knife to the volume of the ring knife is the density of the soil. The compression modulus was determined from oedometer tests which is the ratio of the vertical stress increment to the corresponding strain increment of the soil under the lateral limit. The moisture content was obtained from moisture content tests. The sample was placed in an oven with a temperature of 105–110°C; the temperature can be adjusted by the control button of the oven. The ratio of the lost water quality when baked to a constant amount to the dry soil quality after reaching a constant amount is the moisture content of the soil. The liquid limit and plastic limit were obtained by liquid limit and plastic limit tests. A balance cone with a mass of 76 g and a cone angle of 30° was used to determine the liquid limit. When the immersion depth of the balance cone was 17 mm, the corresponding moisture content was the liquid limit. The plastic limit was determined by the rolling method; the soil was rolled on a glass plate. During the process of slow and unilateral rubbing, the moisture in the paste evaporates gradually. For example, when the diameter of the soil bar was about 3 mm, cracks occurred and the soil broke into several sections. At this time, the moisture content of the sample was the plastic limit. The cohesion and internal friction angles were determined from direct shear tests. At least 4 specimens were cut and destroyed under different normal stress levels, and the relationship between the shear strength and the normal stress was determined. For clay, this relationship is approximately linear. The angle between the straight line and the transverse axis is the internal friction angle, and the intercept on the longitudinal axis is the cohesive force. The main physical properties of the clay are shown in Table 1.

Since moisture contents in the test area are mainly distributed between 13% and 21%, soil samples with moisture contents of 13%, 15%, 17%, 19%, and 21% were used. When the piles are built in the area with different soil or moisture contents, the design analysis can still be carried out according to the method of this experiment. The elastic modulus of the concrete was 30 GPa. Four concrete surface treatments were tested: no treatment (model 1), coating with a paraffin-oil mixture (model 2), coating with polymer nanomaterial (model 3), and coating with paint (model 4) (Figure 4). There was a 2-mm layer of adhesive between the concrete and coating. Because the thickness of the asphalt coating is 4-5 mm in practical engineering, the thickness of the coating in this study was 4 mm.

2.3. Test Procedure

(1) Model A was put on the pedestal; the prefabricated concrete blocks were placed on top of model A.

(2) Model B was placed on model A and the soil was placed on model B. Because the density of the soil

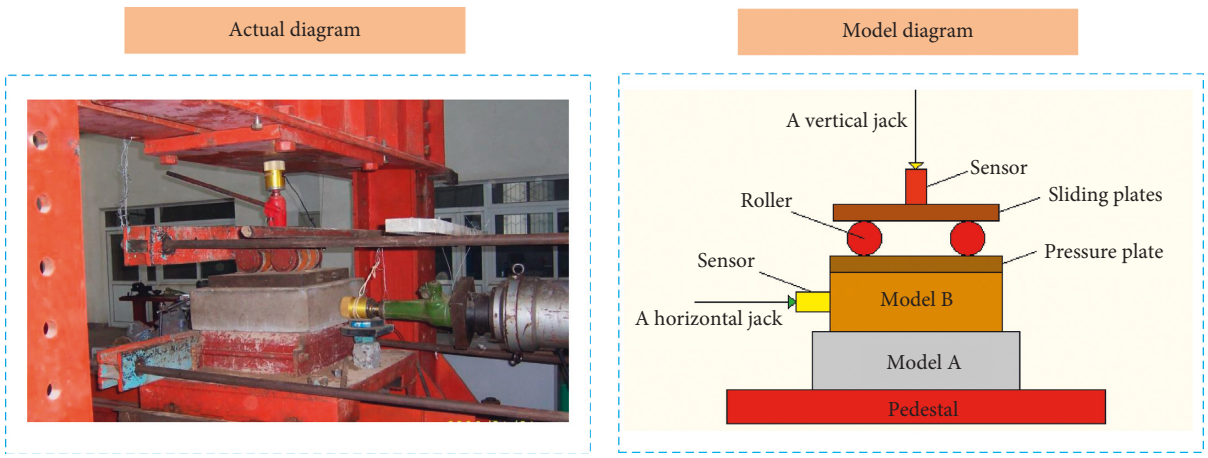

Figure 1: Test equipment of large-scale shear test.

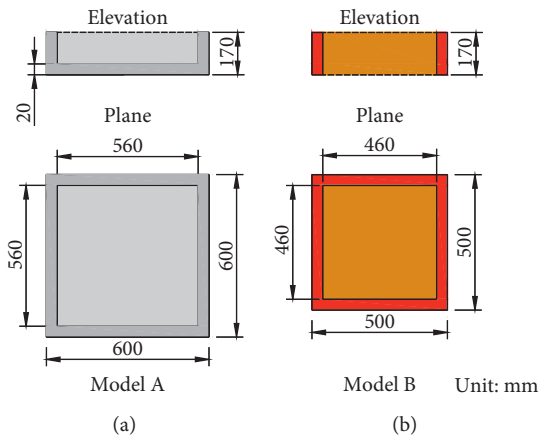

Figure 2: Model dimensions.

Figure 3: Continued.

(c)

(d)

(e)

Figure 3: (a) Ring knife tests; (b) oedometer tests; (c) moisture content tests; (d) liquid limit and plastic limit tests; (e) direct shear tests.

Table 1: Physical properties of clay.

Type	Clay
Density (g/cm^3)	1.7
Compressive modulus (MPa)	11
Moisture content (%)	13
Liquid limit (%)	36
Plastic limit (%)	18
Cohesion (kPa)	22
Internal friction angle (°)	25

sample was 1.7 g/cm^3 and the capacity of model B was 35972 cm^3, 61152.4 g of soil was compressed into model B. The moisture content of the soil sample was 13% and the amount of soil and water in the soil were 54117.2 g and 7035.2 g, respectively (see equations (1) and (2)). Since the required soil moisture content was 15%, it was calculated that the water required in the soil was 8117.6 g. The initial 61152.4 g of soil contained 7035.2 g water; therefore, it was necessary to add 1082.4 g of water to the soil. The method of adjusting the moisture content of the soils was the same for the other samples.

(3) The pressure plate, roller, and sliding plate were placed on top of model B in turn.

(4) The vertical jack and sensor were placed on the sliding plates, and the horizontal jack and sensor were placed on the side of model B.

(5) The vertical load of this study was 10 kN, 20 kN, and 30 kN. Under each load level, a shear load was applied in the horizontal direction until shear failure occurred, at which time the horizontal force value was recorded.

(6) The concrete surface of model 2 was coated with the paraffin-oil mixture, the concrete surface of model 3 was coated with the polymer nanomaterial, and the concrete surface of model 4 was coated with the paint. The remaining steps were the same as above.

$$\omega = m_w \div m_s \times 100\%, \quad (1)$$

where ω is the moisture content of the soil; m_w is the amount of water in the soil; and m_s is the amount of soil particles.

$$m = m_w + m_s + m_a, \quad (2)$$

where m is the total amount of the soil; m_w is the amount of water in the soil; m_s is the amount of soil particles; and m_a is the amount of air in the soil, which is neglected in this study.

3. Results of Friction Strength and Friction Coefficient

In the large-scale shear test, different vertical forces represent the horizontal force on the pile side at different depths

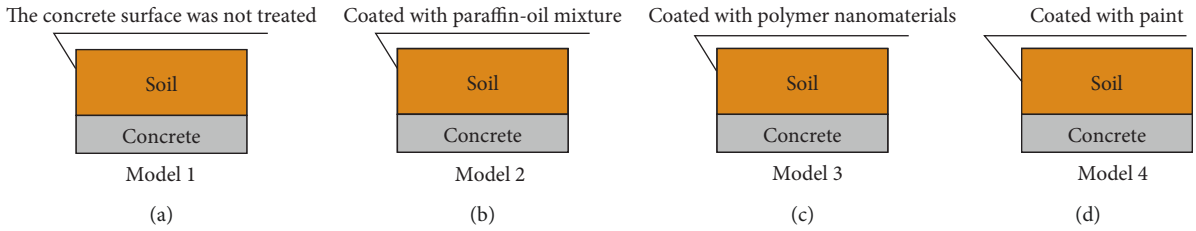

Figure 4: Four concrete surface treatments (models).

of the pile. The principle of shear stress generation in the direct shear test is consistent with the principle of negative skin friction, which occurs due to the relative motion of the two interfaces; therefore, the friction strength represents the negative skin friction of the piles. The friction coefficient is the ratio of the horizontal force to the vertical force or the friction strength to the compressive stress. The test results are shown in Tables 2 to 5.

Due to manual measurement and equipment errors, the friction coefficient varies under different vertical forces. Therefore, the average friction coefficient was used to evaluate the ability of different materials to reduce the negative skin friction between the piles and soil. The friction strength and friction coefficient of clay and concrete with different surface treatments and different moisture content are analyzed. Subsequently, the influences of the moisture content and coatings on the ability to reduce the negative skin friction of the piles are evaluated.

4. Discussion

4.1. Friction Strength of Concrete and Soil for Different Moisture Contents. The frictional strength of the clay with different moisture contents and the untreated concrete is shown in Figure 5.

The results in Figure 5 indicate that when the moisture content of the experimental clay exceeds the plastic limit, the friction strength does not substantially decrease with the increase in the moisture content. When the moisture content of the experimental clay is less than that of the plastic limit, the friction strength increases rapidly with the decrease in the moisture content. At a moisture content of less than 15%, the friction strength does not substantially increase as the moisture content decreases at a vertical force of 10 kN. That is to say, when the vertical force is small and the concrete pile does not have any coating, the negative skin friction of the pile is small when the moisture content of the clay is near or exceeds the plastic limit.

4.2. Friction Strength of the Paraffin-Oil Mixture and Soil for Different Moisture Contents. The frictional strength between the clay for different moisture contents and the concrete coated with the paraffin-oil mixture is shown in Figure 6.

When the vertical pressure is small, the frictional strength is barely affected by the change in the moisture content. The friction strength is the largest at a moisture content of 15% and vertical forces of 10 kN and 30 kN; the reason is that the clay and the paraffin-oil mixture have the largest frictional resistance at this moisture content. At a moisture content of less than 15%, the friction strength increases with the increase in the moisture content. When the moisture content is greater than 15%, the friction strength decreases with the increase in the moisture content for the vertical forces of 10 kN and 30 kN. At a vertical force of 20 kN, the trend of the frictional strength is slightly different at a moisture content of about 17%, which may be due to a measurement error. These results indicate that the ability to reduce the negative skin friction of the piles is greatest when the moisture content of the clay is small or near the plastic limit when a paraffin-oil mixture is applied to the pile.

4.3. Friction Strength of Polymer Nanomaterials and Soil for Different Moisture Contents. The frictional strength between the clay with different moisture contents and the concrete coated with the polymer nanomaterial is shown in Figure 7.

When the moisture content is less than 15%, the friction strength does not change with increasing moisture content. At a moisture content of more than 15%, the friction strength decreases rapidly with the increase in the moisture content. These results demonstrate that the ability to reduce the negative skin friction of the piles is greatest when the moisture content of the clay exceeds the plastic limit when the polymer nanomaterial is applied to the pile.

4.4. Friction Strength of Paint and Soil for Different Moisture Contents. The frictional strength between the clay with different moisture contents and the concrete coated with paint is shown in Figure 8.

When the moisture content of the experimental clay exceeds the plastic limit, the frictional strength is not affected by the change in the moisture content. When the moisture content is less than that of the plastic limit, the friction strength increases rapidly with the decrease in the moisture content. At a moisture content of less than 15%, the friction strength does not substantially increase as the moisture content decreases. The results show that the ability to reduce the negative skin friction of the piles is greatest when the moisture content of the clay is near the plastic limit when paint is applied to the pile.

4.5. Friction Coefficient between Various Coatings and the Soil for Different Moisture Contents. As is shown in Tables 2 to 5, when the same treatments are applied to the concrete surface of the pile and the moisture content remains unchanged, the

Table 2: Model 1.

Moisture content (%)	Vertical force (kN)	Compressive stress (kPa)	Horizontal force (kN)	Friction strength (kPa)	Friction coefficient	Average friction coefficient
	10	47.26	3.09	14.60	0.310	
21	20	94.52	6.22	29.40	0.311	0.31
	30	141.78	9.34	44.14	0.311	
	10	47.26	3.32	15.69	0.332	
19	20	94.52	7.53	35.59	0.376	0.35
	30	141.78	9.93	46.93	0.331	
	10	47.26	4.88	23.06	0.488	
17	20	94.52	8.39	39.65	0.420	0.45
	30	141.78	13.49	63.75	0.450	
	10	47.26	6.75	31.90	0.675	
15	20	94.52	13.12	62.00	0.656	0.64
	30	141.78	17.98	84.97	0.599	
	10	47.26	6.81	32.18	0.681	
13	20	94.52	15.52	73.35	0.776	0.70
	30	141.78	18.91	89.37	0.630	

Table 3: Model 2.

Moisture content (%)	Vertical force (kN)	Compressive stress (kPa)	Horizontal force (kN)	Friction strength (kPa)	Friction coefficient	Average friction coefficient
	10	47.26	1.49	7.04	0.149	
21	20	94.52	2.80	13.23	0.140	0.15
	30	141.78	4.42	20.89	0.147	
	10	47.26	2.58	12.19	0.258	
19	20	94.52	4.44	20.98	0.222	0.23
	30	141.78	6.03	28.50	0.201	
	10	47.26	2.83	13.37	0.283	
17	20	94.52	5.84	27.60	0.292	0.27
	30	141.78	7.13	33.70	0.238	
	10	47.26	2.93	13.85	0.293	
15	20	94.52	5.79	27.36	0.290	0.29
	30	141.78	8.72	41.21	0.291	
	10	47.26	2.60	12.29	0.260	
13	20	94.52	4.35	20.56	0.217	0.23
	30	141.78	6.15	29.06	0.205	

Table 4: Model 3.

Moisture content (%)	Vertical force (kN)	Compressive stress (kPa)	Horizontal force (kN)	Friction strength (kPa)	Friction coefficient	Average friction coefficient
	10	47.26	1.17	5.53	0.117	
21	20	94.52	2.84	13.42	0.142	0.13
	30	141.78	4.28	20.23	0.143	
	10	47.26	2.71	12.81	0.271	
19	20	94.52	4.73	22.35	0.237	0.25
	30	141.78	6.85	32.37	0.228	
	10	47.26	4.09	19.33	0.409	
17	20	94.52	7.72	36.48	0.386	0.39
	30	141.78	11.12	52.55	0.371	
	10	47.26	5.06	23.91	0.506	
15	20	94.52	10.40	49.15	0.520	0.51
	30	141.78	15.02	70.98	0.501	
	10	47.26	5.30	25.05	0.530	
13	20	94.52	10.57	49.95	0.529	0.53
	30	141.78	15.76	74.48	0.525	

Table 5: Model 4.

Moisture content (%)	Vertical force (kN)	Compressive stress (kPa)	Horizontal force (kN)	Friction strength (kPa)	Friction coefficient	Average friction coefficient
	10	47.26	2.12	10.02	0.212	
21	20	94.52	4.94	23.35	0.247	0.22
	30	141.78	5.88	27.79	0.196	
	10	47.26	2.65	12.52	0.265	
19	20	94.52	4.85	22.92	0.243	0.25
	30	141.78	7.07	33.41	0.236	
	10	47.26	3.17	14.98	0.317	
17	20	94.52	6.56	31.00	0.328	0.32
	30	141.78	9.72	45.94	0.324	
	10	47.26	5.42	25.61	0.542	
15	20	94.52	10.56	49.91	0.528	0.55
	30	141.78	17.16	81.10	0.572	
	10	47.26	6.26	29.58	0.626	
13	20	94.52	10.98	51.89	0.549	0.61
	30	141.78	19.50	92.16	0.650	

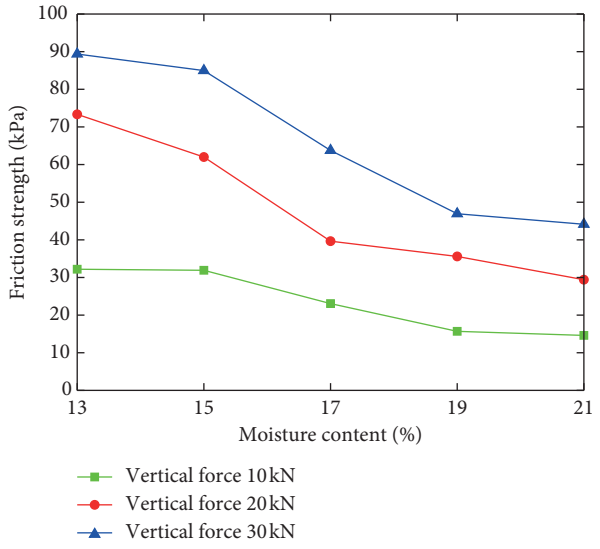

Figure 5: Friction strength of concrete and soil for different moisture contents.

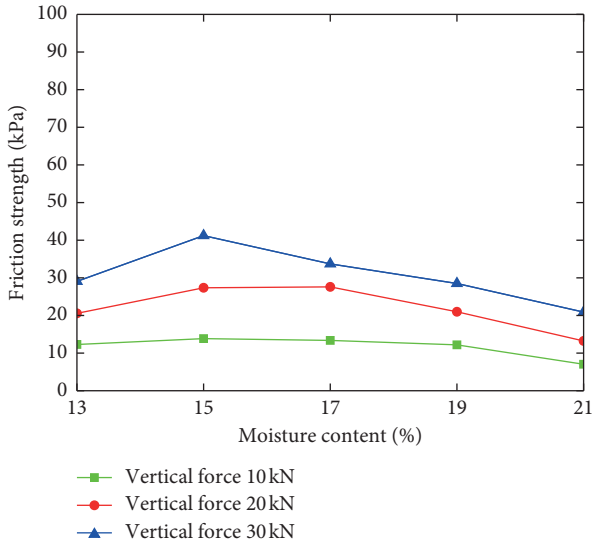

Figure 6: Friction strength of the paraffin-oil mixture on the concrete surface and soil for different moisture contents.

change in the vertical force hardly changes the friction coefficient between the pile and soil. The average friction coefficients between the experimental clay and the concrete treated with different coatings for different moisture contents are compared in Figure 9.

For concrete with coating, when the moisture content is 13%–15%, the reduction effect of the paraffin-oil mixture is the best, and the reduction effect of the paint is the worst; When the moisture content is 15%–19%, the reduction effect of the paraffin-oil mixture is the best, and the reduction effect of the polymer nanomaterial is mostly the worst; when the moisture content is 19%–21%, the paraffin-oil mixture and polymer nanomaterial have better reduction effects, and the reduction effect of the paint is the worst.

It is observed that the friction coefficient can be reduced by applying the paraffin-oil mixture, polymer nanomaterial, or paint on the surface of the concrete. This indicates that these treatments on the concrete surface reduce the negative skin friction of the piles.

The most effective treatment to reduce the negative skin friction of the piles is to coat the concrete surface with the paraffin-oil mixture. In addition, a paraffin-oil mixture is relatively common. It should be the first choice for reducing the negative skin friction of the piles in engineering practice.

The reduction in the negative skin friction for the polymer nanomaterial coating on the concrete surface is greater at a moisture content of less than 15% or when the plastic limit has been exceeded.

The friction coefficient of the concrete coated with paint shows changes that are similar to that of the untreated concrete. When the moisture content is near the plastic limit, the friction coefficient changes abruptly and there are only small changes when the moisture content is far from the plastic limit. Therefore, when the surface of the concrete pile is coated with paint, the moisture content should be slightly

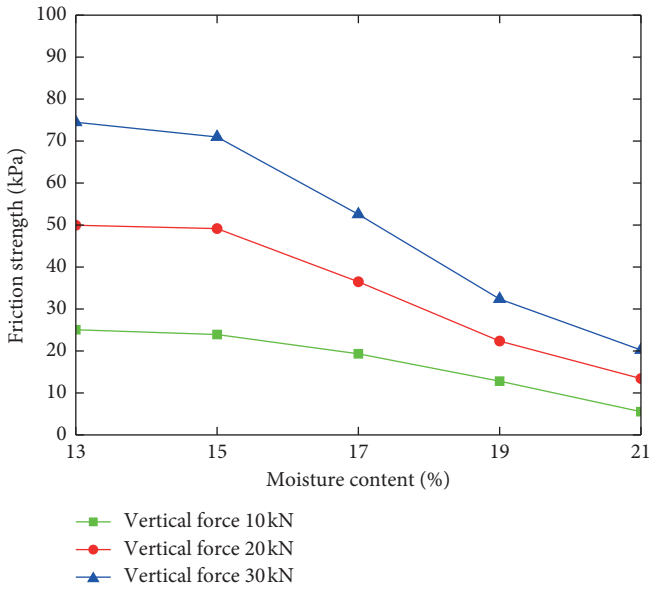

Figure 7: Friction strength of the polymer nanomaterial on the concrete surface and soil for different moisture contents.

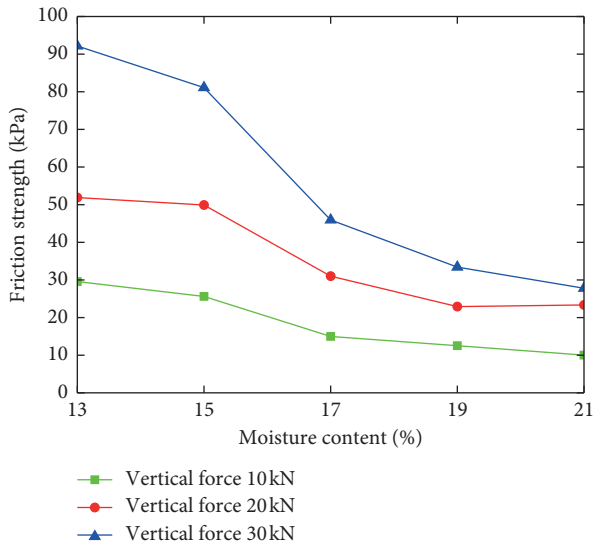

Figure 8: Friction strength of paint on the concrete surface and soil for different moisture contents.

larger than that of the plastic limit to reduce the negative skin friction of the piles.

A comparison of the effects of the three kinds of coatings and the different moisture contents shows that when the moisture content is slightly larger than that of the plastic limit, the three coatings exhibit similar performance for reducing the negative skin friction. Overall, the paraffin-oil mixture results in the best performance.

As shown in Table 6, the largest reduction rate of the average friction coefficient is achieved for the polymer nanomaterial coating at a moisture content of 21%. The largest reduction rate for the paraffin-oil mixture is achieved at a moisture content of 21%, but overall, the average friction coefficient for the paraffin-oil mixture and

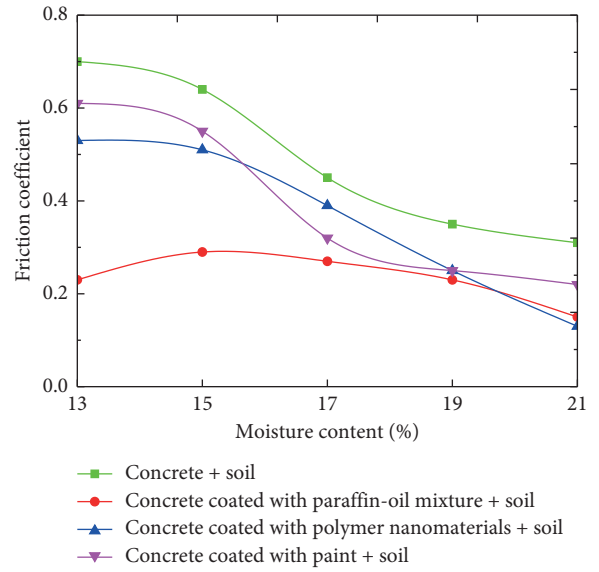

Figure 9: Friction coefficients of concrete with various coatings and soil for different moisture contents.

soil is almost unaffected by changes in the moisture content. When the moisture content is slightly larger than that of the plastic limit, the three coatings have similar effects on the reduction rate of the average friction coefficient. The paraffin-oil mixture provides the best performance in terms of reducing negative skin friction. The reduction rate of the average friction coefficient is calculated using the following equation:

$$\alpha_t = \frac{F_{t0} - F_{ti}}{F_{t0}}, \tag{3}$$

where α_t is the reduction rate of the average friction coefficient, F_{t0} is the average friction coefficient between concrete and soil, and F_{ti} is the average friction coefficient between concrete coated with different coatings and soil.

4.6. Measures to Reduce Negative Skin Friction of Piles. The location of the neutral point is important for the reduction in the negative skin friction of the piles with different coatings. The position of the neutral point can be determined by theoretical calculation methods and empirical methods. The most common method is the empirical method [34]; the neutral point depth based on this method is shown in Table 7.

The coating should be applied to the pile above the location of the neutral point, as shown in the schematic of the construction process in Figure 10. The test results indicate that when the moisture content of the clay is near the plastic limit, the effect of applying the paraffin-oil mixture, the polymer nanomaterial, or the paint on the concrete surface is similar, and all coatings can be used to reduce negative skin friction of the piles. However, the paraffin-oil mixture is the first choice as a coating when there is a large difference between the moisture content of the clay and the plastic limit.

Table 6: Reduction rate of average friction coefficient.

Moisture content (%)	Reduction rate of average friction coefficient α_t (%)		
	Paraffin-oil mixture	Polymer nanomaterial	Paint
13	67.14	24.29	12.86
15	58.57	27.14	21.43
17	61.43	44.29	54.29
19	67.14	64.29	64.29
21	78.57	81.43	68.57

Table 7: Neutral point depth.

Force layer properties	Clay, powder soil	Sand above medium density	Self-weight collapsible loess	Gravel, pebble	Bedrock
Depth ratio of neutral point L_n/L_0	0.5–0.6	0.7–0.8	0.77–0.8	0.9	1.0

Note. L_n and L_0 are the depth of the neutral point and the lower limit depth of the settlement and the deformation soil layer in the area surrounding the pile, respectively.

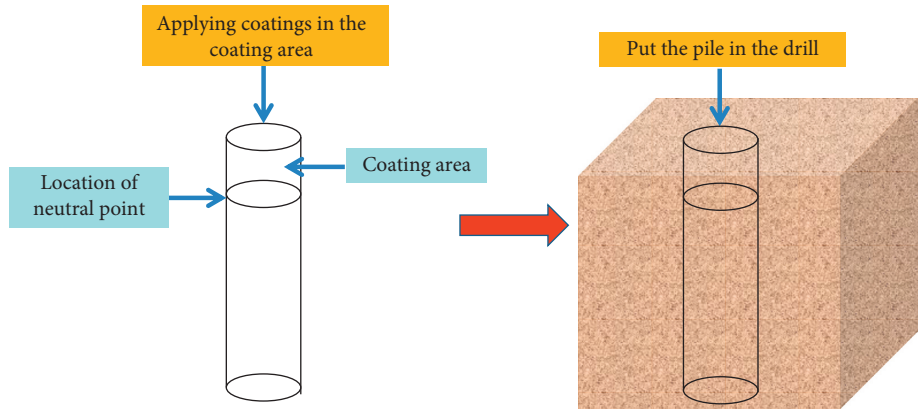

Figure 10: Schematic of the construction process.

5. Conclusions

In this study, the effects of different coatings on the ability to reduce negative skin friction on piles during a large-scale shear test were examined. The following conclusions were drawn:

(1) When the moisture content of the clay was slightly larger than that of the plastic limit, the negative skin friction of the piles could be reduced considerably.

(2) Different coatings exhibited different degrees of reduction of the negative skin friction of piles; the performance of the paraffin-oil mixture was the best when the moisture content of the clay was lower than that of the plastic limit.

(3) When the moisture content of the clay was near the plastic limit, the performances of the paraffin-oil mixture, polymer nanomaterial, or paint were similar and all coatings reduced the negative skin friction. The paraffin-oil mixture is the best choice when the moisture content of the clay is lower than that of the plastic limit.

Data Availability

The data used to support the findings of this study are available from the corresponding author upon request.

Conflicts of Interest

The authors declare no conflicts of interest.

Acknowledgments

This research was funded by the National Key Research and Development Program of China (no. 2018YFC1504801); Traffic Science and Technology Projects in Guangdong Province (2013-02-010 and 2011-01-001); Key Transportation Science and Technology Research Projects in Qinghai Province (2014-07); and Traffic Science and Technology Projects in Hainan Province (HNZXY2015-045R).

References

[1] J. Lai, H. Liu, J. Qiu et al., "Stress analysis of CFG pile composite foundation in consolidating saturated mine tailings dam," *Advances in Materials Science and Engineering*, vol. 2016, Article ID 3948754, 12 pages, 2016.

[2] Z. Zhou, Y. Dong, P. Jiang, D. Han, and T. Liu, "Calculation of pile side friction by multiparameter statistical analysis," *Advances in Civil Engineering*, vol. 2019, p. 12, 2019.

[3] H. Sun, Q. P. Wang, P. Zhang, Y. J. Zhong, and X. B. Yue, "Spatialtemporal characteristics of tunnel traffic accidents in

China from 2001 to present," *Advances in Civil Engineering*, vol. 2019, Article ID 4536414, 16 pages, 2019.

[4] T. Liu, Y. J. Zhong, Z. H. Feng, W. Xu, and F. T. Song, "New construction technology of a shallow tunnel in boulder-cobble mixed grounds," *Advances in Civil Engineering*, vol. 2020, Article ID 5686042, 14 pages, in Press.

[5] J. Lai, H. Liu, J. Qiu, and J. Chen, "Settlement analysis of saturated tailings dam treated by CFG pile composite foundation," *Advances in Materials Science and Engineering*, vol. 2016, Article ID 7383762, 10 pages, 2016.

[6] Q. Q. Zhang, L. P. Li, and Y. J. Chen, "Analysis of compression pile response using a softening model, a hyperbolic model of skin friction, and a bilinear model of end resistance," *Journal of Engineering Mechanics*, vol. 140, no. 1, pp. 102–111, 2013.

[7] Z. Zhou, S. Zhu, X. Kong, J. Lei, and T. Liu, "Optimization analysis of settlement parameters for postgrouting piles in loess area of Shaanxi, China," *Advances in Civil Engineering*, vol. 2019, Article ID 7085104, 16 pages, 2019.

[8] Z. Feng, H. Hu, Y. Dong et al., "Effect of steel casing on vertical bearing characteristics of steel tube-reinforced concrete piles in loess area," *Applied Sciences*, vol. 9, no. 14, p. 2874, 2019.

[9] T. Huang, W. Gong, and G. Dai, "Model tests on characteristics of pile foundation negative skin friction under different distributions of surcharge load," *Journal of Southeast University*, vol. 45, 2015.

[10] H.-J. Kim, J. L. Mission, T.-W. Park, and P. R. Dinoy, "Analysis of negative skin-friction on single piles by one-dimensional consolidation model test," *International Journal of Civil Engineering*, vol. 16, no. 10, pp. 1445–1461, 2018.

[11] J. Qiu, X. Wang, J. Lai, Q. Zhang, and J. Wang, "Response characteristics and preventions for seismic subsidence of loess in Northwest China," *Natural Hazards*, vol. 92, no. 3, pp. 1909–1935, 2018.

[12] J. J. Sun, L. M. Wang, and X. F. Huang, "A study on the position of maximum negative skin friction on piles in collapsing loess ground," *Journal of Seismology*, vol. 23, 2003.

[13] S. Jeong, J. Ko, C. Lee, and J. Kim, "Response of single piles in marine deposits to negative skin friction from long-term field monitoring," *Marine Georesources & Geotechnology*, vol. 32, no. 3, pp. 239–263, 2014.

[14] H. Xing and L. Liu, "Field tests on influencing factors of negative skin friction for pile foundations in collapsible loess regions," *International Journal of Civil Engineering*, vol. 16, no. 10, pp. 1413–1422, 2018.

[15] B. H. Fellenius, "Down-drag on piles in clay due to negative skin friction," *Canadian Geotechnical Journal*, vol. 9, no. 4, pp. 323–337, 1972.

[16] I. Mashhour and A. Hanna, "Drag load on end-bearing piles in collapsible soil due to inundation," *Canadian Geotechnical Journal*, vol. 53, no. 12, pp. 2030–2038, 2016.

[17] M. Uesugi and H. Kishida, "Frictional resistance at yield between dry sand and mild steel," *Soils and Foundations*, vol. 26, no. 4, pp. 139–149, 1986.

[18] H. G. Poulos, "Cyclic axial loading analysis of piles in sand," *Journal of Geotechnical Engineering*, vol. 115, no. 6, pp. 836–852, 1989.

[19] H. J. Pincus, J. T. Tabucanon, D. W. Airey, and H. G. Poulos, "Pile skin friction in sands from constant normal stiffness tests," *Geotechnical Testing Journal*, vol. 18, no. 3, pp. 350–364, 1995.

[20] R. C. Chaney, K. R. Demars, H. A. Joer, M. F. Randolph, and U. Gunasena, "Experimental modeling of the shaft capacity of grouted driven piles," *Geotechnical Testing Journal*, vol. 21, no. 3, pp. 159–168, 1998.

[21] M. K. Kim, J. S. Lee, and M. K. Kim, "Vertical vibration analysis of soil-pile interaction systems considering the soil-pile interface behavior," *KSCE Journal of Civil Engineering*, vol. 8, no. 2, pp. 221–226, 2004.

[22] B. Ampera and T. Aydogmus, "Skin friction between peat and silt soils with construction materials," *Electronic Journal of Geotechnical Engineering*, vol. 10, p. 13, 2005, https://www.researchgate.net/publication/289830705_Skin_Friction_between_Peat_and_Silt_Soils_with_Construction_Materials.

[23] W. Cao, Y. Chen, and W. Wolfe, "New load transfer hyperbolic model for pile-soil interface and negative skin friction on single piles embedded in soft soils," *International Journal of Geomechanics*, vol. 14, no. 1, pp. 92–100, 2013.

[24] A. D. Donna, A. Ferrari, and L. Laloui, "Experimental investigations of the soil–concrete interface: physical mechanisms, cyclic mobilization, and behaviour at different temperatures," *Canadian Geotechnical Journal*, vol. 53, no. 4, pp. 659–672, 2016.

[25] S. Bersan, O. Bergamo, L. Palmieri, L. Schenato, and P. Simonini, "Distributed strain measurements in a CFA pile using high spatial resolution fibre optic sensors," *Engineering Structures*, vol. 160, pp. 554–565, 2018.

[26] B. H. Fellenius, "Reducing negative SKIN friction with bitumen slip layers," *Journal of Geotechnical & Geoenvironmental Engineering*, vol. 101, no. GT4, 1975, https://trid.trb.org/view/39091.

[27] N. S. Kurnoskina, "Use of antifriction coatings for reducing friction between pile lateral surfaces and soil," *Soil Mechanics and Foundation Engineering*, vol. 20, no. 6, pp. 236–239, 1983.

[28] K. S. Tawfiq and J. A. Caliendo, "Bitumen coating versus plastic sheeting for reducing negative skin friction," *Journal of Materials in Civil Engineering*, vol. 7, no. 1, pp. 69–81, 1995.

[29] B. H. Fellenius, "Bitumen selection for reduction of downdrag on piles," *Journal of Geotechnical and Geoenvironmental Engineering*, vol. 125, no. 4, pp. 341–344, 1999.

[30] M. G. Khare and S. R. Gandhi, "Skin friction of piles coated with bituminous coats," *Contemporary Issues in Deep Foundations*, 2007.

[31] B. Rahimzadeh, *Linear and Non-Linear Viscoelastic Behaviour of Binders and Asphalts*, Ph.D. thesis, University of Nottingham, Nottingham, UK, 2002.

[32] R. Taylor, *Surface Interactions between Bitumen and Mineral Filling and Their Effects on the Rheology of Bitumen-Filler Mastics*, Ph.D. thesis, University of Nottingham, Nottingham, UK, 2007.

[33] J. Yi, S. Shen, B. Muhunthan, and D. Feng, "Viscoelastic–plastic damage model for porous asphalt mixtures: application to uniaxial compression and freeze–thaw damage," *Mechanics of Materials*, vol. 70, pp. 67–75, 2014.

[34] Ministry of Housing and Urban-Rural Construction of the People's Republic of China., *Chinese Technical Code for Building Pile Foundations JGJ94-2008*, China Architecture & Building Press, Beijing, China, 2008, in Chinese.